LIQUEFACTION-DEPENDENT FRAGILITY RELATIONSHIPS OF COMPLEX BRIDGE-FOUNDATION-SOIL SYSTEMS

Oh-Sung Kwon [1], Anastasios Sextos [2] and Amr S. Elnashai [3]

[1] *Post-Doctoral Research Associate, Department of Civil and Environmental Engineering, University of Illinois at Urbana-Champaign, Urbana, IL, USA, E-mail: okwon2@uiuc.edu*

[2] *Lecturer, Civil Engineering Department, Aristotle University Thessaloniki, Greece*

[3] *Bill and Elaine Hall Endowed Professor, Director of the Mid-America Earthquake Centre, University of Illinois at Urbana-Champaign, Urbana, IL,, USA*

ABSTRACT: This paper presents the development of liquefaction-sensitive fragility curves for a bridge-foundation-soil system. A refined computational scheme is implemented for this purpose involving both a 3-dimentional inelastic multi-platform model and an appropriately calibrated simplified model supported on nonlinear foundation springs. Artificial and natural, near- and far-field, earthquake records are used to account for input motion uncertainty while uniform and non-uniform soil conditions along the bridge length are assumed for the central pier and the abutments of the bridge. The results of the study indicate that the inelastic dynamic response of such systems maybe significantly affected by the liquefaction of upper soil layers. Moreover, it is shown that the spatial extent of liquefaction is an additional parameter that has to be considered as an important source of ground motion and ductility demand variation.

1. INTRODUCTION

The impact of an earthquake on the performance of a highway transportation network depends on the extent of damage sustained by its individual components, particularly bridges. This critical seismic vulnerability of bridges is often described by fragility curves which express the conditional probability that a bridge will exhibit certain damage states, subject to the intensity of the earthquake. The complexity and computational cost of modeling the inelastic response of the superstructure hampers the development of equally refined finite element models to consider the role played by the foundation and the supporting soil in terms of incident ground motion modification, local (at each foundation) radiation and material damping as well as changes in structural dynamic characteristics. Due to this complexity, the computationally intensive case of soil liquefaction susceptibility at certain depths below the bridge foundation and its overall effect on the dynamic response of soil-foundation-superstructure systems is commonly ignored. The scope of this paper therefore is to investigate the importance of considering the liquefaction potential of soils in the vulnerability analysis process for bridges supported on loose-to-moderate saturated cohesionless soils. Along these lines, the well-studied (Zhang and Makris, 2001; Kwon, 2007) Meloland Road Overcorssing (MRO) bridge is adopted for the current study. The bridge was built in 1971 and is located over Interstate 8 approximately 0.5 km from the fault rupture of the 1979 Imperial Valley earthquake. The bridge consists of two spans of pre-stressed box-girder decks monolithically connected to the center pier. The abutments are placed on fill. Seven piles support each abutment. Each side of abutment has 5.9 m of wing-wall. The pier at the center of the bridge has a diameter of 1.5 m and is 7.9 m is high from the top of piles. A total of 18 longitudinal reinforcement bars are used in the pier, the foundations of which are supported on 25 timber piles spaced at 0.91 m. The procedure of earthquake selection, site response and liquefaction consideration, analysis environment and vulnerability assessment is presented below.

2. GENERATION AND SELECTION OF EARTHQUAKE GROUND MOTIONS

2.1 Generation of artificial ground motions

As a means to consider and quantify the inherent uncertainty of earthquake ground motion, six levels of ground motion intensity are established for the fragility analysis, i.e., 0.05g, 0.1g, 0.2g, 0.3g, 0.4g, 0.5g, all assumed at the bedrock level. It is worth noting that in contrast to a typical vulnerability assessment process, it is necessary to select (or generate) intensity compatible

motions at the bedrock level in order to consider the effect of strain softening of particular layers under cyclic loading during upward seismic wave propagation. In total, 18 artificial records were first generated at the bedrock level, corresponding to three surface Magnitudes (6.0, 6.5 and 7.0). Records at the bedrock level were generated as white noise emanating from the earthquake source using Monte-Carlo simulations for stationary processes (Manolis et al., 2007) and were rendered non-stationary through use of time envelope functions. Records were filtered through a Kanai-Tajimi (KT) filter, a high-pass (HP) filter, and a low-pass (LP) filter. The Magnitude-dependent filter values were derived according to Papageorgiou and Aki (1983). Peak ground acceleration was correlated to white noise intensity S_0 according to Shinozuka (1987) and to distance R, using the McGuire (1978) attenuation relationship for distances up to 15km and that of Ambrasseys and Douglas (2000) for the rest. The duration was also considered as a variable, according to the corresponding magnitude M and epicentral distance R. This is a critical parameter which was taken to vary on purpose since it is a significant part of strong motion that affects the maximum response when a structure undergoes inelastic deformations. From the numerous definitions of strong ground motion duration, the 'significant duration' was used, appropriately modified by a factor of 1.3 in order to derive the total signal duration required for the modulating (time envelope) function. It is noted that despite of the convenience of the Kanai-Tajimi power spectrum, by numerous researchers have stressed its inability to consider the high frequency content of near field motions. Nevertheless, the reason that it was adopted in the present study is that, notwithstanding its limitations, it provides a well controlled by the user incremental level of earthquake intensity and hence, the target bedrock PGA of 0.05g, 0.1g, 0.2g, 0.3g, 0.4g and 0.5g is achieved in a smooth way appropriate for fragility analysis. However, in order to counteract to a certain extent the above limitation to represent near-field motions, the frequency and damping of the HP filter were appropriately modified for all records assumed at distances R < 20km (i.e. a double frequency ω_g and a 20% reduced value of damping ξ_g was adopted).

2.2 Selection of natural records

As a means to complement the artificially generated ground motions, it was deemed necessary to select an additional set of 18 records, from a large database of available recordings (https://peer.berkeley.edu). Effort was made to select motions representative in terms of (rock) soil conditions and target intensity levels (0.05g, 0.1g, 0.2g, 0.3g, 0.4g and 0.5g) in order to be able to use them as bedrock reference motion with only minor scaling. Moreover, both near- and far-field records were sought in order to enrich the earthquake sample and further counteract the inherent limitation of the artificial motion realizations in terms of near-field conditions. The complete list of the earthquake records generated and selected respectively are summarized in Table 1.

2.3 Site response analysis, liquefaction consideration, and analysis scenarios

The ground motions selected were applied at the bedrock level and site response analysis was performed both ignoring and considering liquefaction phenomena. It is also noted that the bedrock was assumed elastic with shear wave properties corresponding to the rock conditions and water table was assumed at the ground surface. Each motion was recorded according to Table 1. The soil column properties underneath the Central Pier are illustrated in Figure 1. A set of reference analyses was first performed corresponding to fully fixed support conditions and completely neglecting sand liquefaction and clay plasticity, thus corresponding to an essentially elastic site response analysis (Case A).

Next, the condition of nonlinear foundation and abutment compliance was considered based on the calibration with purely inelastic models as presented below, but again neglecting the effect of soil liquefaction for comparison purposes (Case B). A more refined representation of soil inelastic behavior was then performed using the multi-yield-surface plasticity model developed by UC San Diego and incorporated into the computer program Cyclic-1D (Elgamal et al., 2002). In the Cyclic-1D, the experimentally observed accumulation of permanent shear strain is modeled by using strain-space parameters and appropriate loading-unloading flow rules which are devised to reproduce the observed strong dilation tendency and the resulting increase in cyclic shear stiffness and strength during earthquake loading. The response at the soil surface was considered as the uniform earthquake foundation input motion for both bridge central pier and abutments (Case C).

Table 1 List of records generated and selected

ID	Earthquake	Location	Ms	R (km)	PGA (g)	Vs (m/sec)
C1	Synthetic	Bedrock	6.0	8.7	0.500	rock
C2	Synthetic	Bedrock	6.0	10.5	0.400	rock
C3	Synthetic	Bedrock	6.0	13.4	0.300	rock
C4	Synthetic	Bedrock	6.0	19.0	0.200	rock
C5	Synthetic	Bedrock	6.0	34.4	0.100	rock
C6	Synthetic	Bedrock	6.0	62.0	0.050	rock
C7	Synthetic	Bedrock	6.5	12.7	0.500	rock
C8	Synthetic	Bedrock	6.5	15.3	0.400	rock
C9	Synthetic	Bedrock	6.5	19.6	0.300	rock
C10	Synthetic	Bedrock	6.5	27.7	0.200	rock
C11	Synthetic	Bedrock	6.5	50.0	0.100	rock
C12	Synthetic	Bedrock	6.5	90.0	0.050	rock
C13	Synthetic	Bedrock	7.0	18.5	0.500	rock
C14	Synthetic	Bedrock	7.0	22.4	0.400	rock
C15	Synthetic	Bedrock	7.0	28.7	0.300	rock
C16	Synthetic	Bedrock	7.0	40.5	0.200	rock
C17	Synthetic	Bedrock	7.0	73.5	0.100	rock
C18	Synthetic	Bedrock	7.0	132.0	0.050	rock
C19	Loma Prieta (1989)	Gilroy Array #1	6.93	28.6	0.473	1428
C20	Loma Prieta (1989)	Gilroy Array #1	6.93	28.6	0.411	1428
C21	Parkfield (1966)	Temblor pre	6.19	40.6	0.300	528
C22	Whittier Narrows (1987)	Mt Wilson - CIT Sta	5.99	19.5	0.186	822
C23	Hollister (1974)	Gilroy Array #1	5.14	11.1	0.105	1428
C24	Loma Prieta (1989)	SF Sierra Pt.	6.93	83.5	0.056	1021
C25	Victoria, Mexico (1980)	Cerro Prieto	6.33	33.7	0.572	659
C26	Loma Prieta (1989)	UCSC Lick	6.93	16.3	0.395	715
C27	Northridge (1994)	Mt Wilson – CIT	6.69	45.8	0.234	821
C28	Northridge (1994)	Wonderland Ave	6.69	18.9	0.172	1222
C29	San Fernando 1971	Lake Hughes #9	6.6	23.0	0.139	671
C30	Northridge (1994)	Antelope Buttes	6.69	63.9	0.046	821
C31	N. Palm Springs (1986)	Whitewater Trout	6.06	4.24	0.492	USGS A
C32	Loma Prieta (1989)	Gilroy-Gavilan Coll	6.93	29.0	0.357	729
C33	Livermore (1980)	Morgan Terr Park	5.42	10.33	0.252	713
C34	Livermore (1980)	Morgan Terr Park	5.42	10.33	0.198	713
C35	Loma Prieta (1989)	Piedmont Jr High	6.93	92.2	0.084	895
C36	Northridge (1994)	Littlerock	6.69	61.2	0.060	821

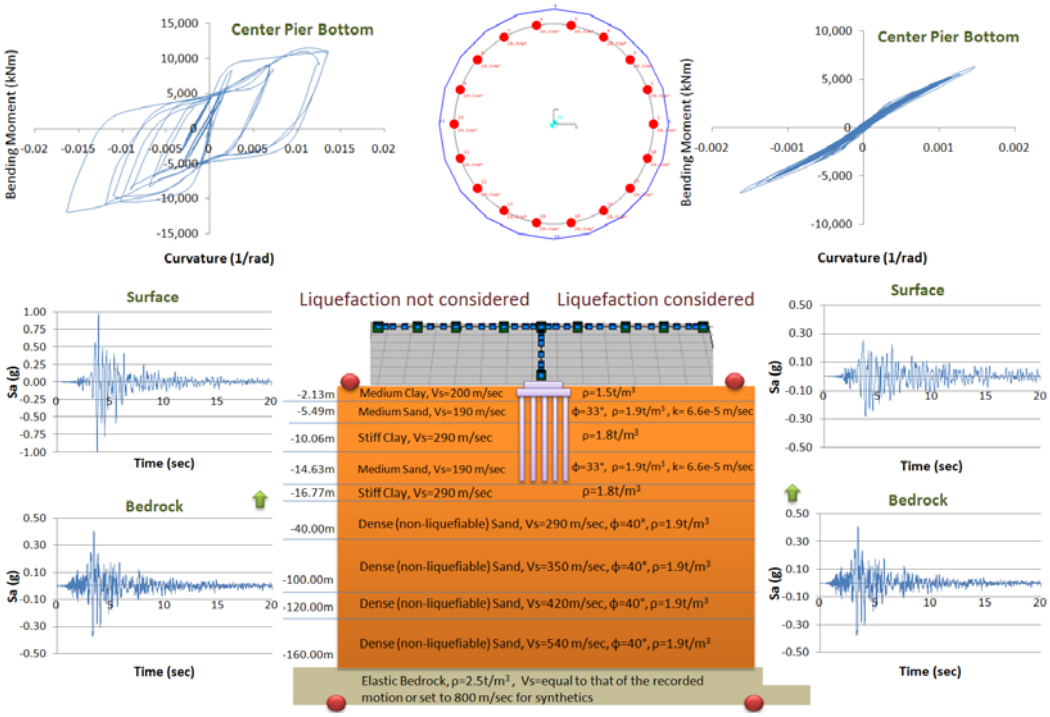

Figure 1 Pier Damage considering (right) and neglecting (left) soil liquefaction. Excitation case: C20

Finally, the scenario that liquefaction occurs only below the central pier was also investigated (Case D), leading to asynchronous excitation of the bridge with support motions corresponding to the liquefaction susceptible soil profile at the central pier and the distinct, non-liquefiable, soil and embankment profile at the abutments. From the site response analyses performed, a significant reduction of the surface PGA was observed for all cases of moderate to high intensity bedrock motion, as a result of a critical acceleration of the upper sand layers which was found approximately equal to 0.25-0.29g (depending on the number of cycles). This acceleration 'cut-off' has resulted in the reduction of the imposed seismic demand at the base of the pier compared to the case where liquefaction was not considered (as shown in Figure 1 for excitation case C20).

3. COMPUTATIONAL FRAMEWORK

Two different finite element models were implemented in order to achieve a balance between analysis accuracy and computational cost for the vulnerability analysis. First, the concept of multi-platform simulation was implemented using the pseudo-dynamic (PSD) simulation approach combined with sub-structuring. In this approach, a structure is subdivided into several modules that are either physically tested or computationally simulated. UI-SimCor (Kwon et al., 2005) was developed in order to coordinate either software or hardware supporting NEESgrid Teleoperation Control Protocol (NTCP) as well as TCP-IP connections outside of the NEES system. It is also capable of using the same analysis platform while modeling different parts of the system on the same or different processors, thus minimizing computing run time. In the particular analysis of the MRO bridge, UI-SimCor was used to enable the concurrent use of two different analysis packages and coordinated four distributed modules in the time domain corresponding respectively to: (a) the bridge sub-system, which was modeled using the verified inelastic dynamic analysis platform ZEUS-NL (Elnashai et al., 2002), (b) the soil-pile foundation sub-system that was analyzed with OpenSees (McKenna and Fenves, 2001), as well as the left (c) and right (d), pile-supported, abutment-embankment system (Figure 2). The particular refined model was used to calibrate the central pier and abutment foundation stiffness of a second, simplified MRO bridge modeled in Zeus-NL as seen in Figure 2. Successful comparison between the dynamic response of the refined 3-D, inelastic multi-platform model and the simplified one used for vulnerability analysis is illustrated in Figure 3. It is noted that the inelastic law adopted for the superstructure concrete sections was common in both models.

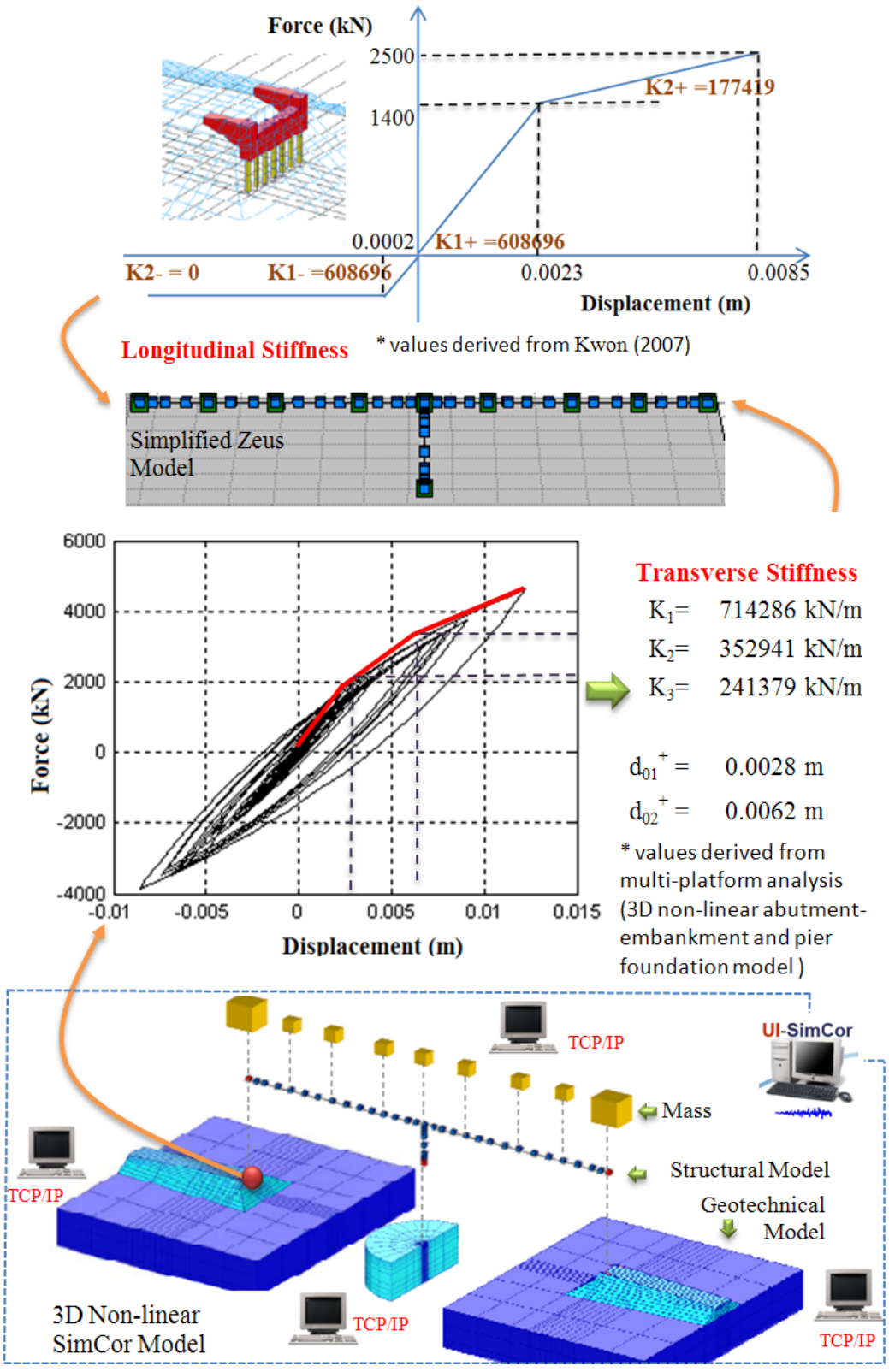

Figure 2 Calibration of simplified model based on multi-platform analysis

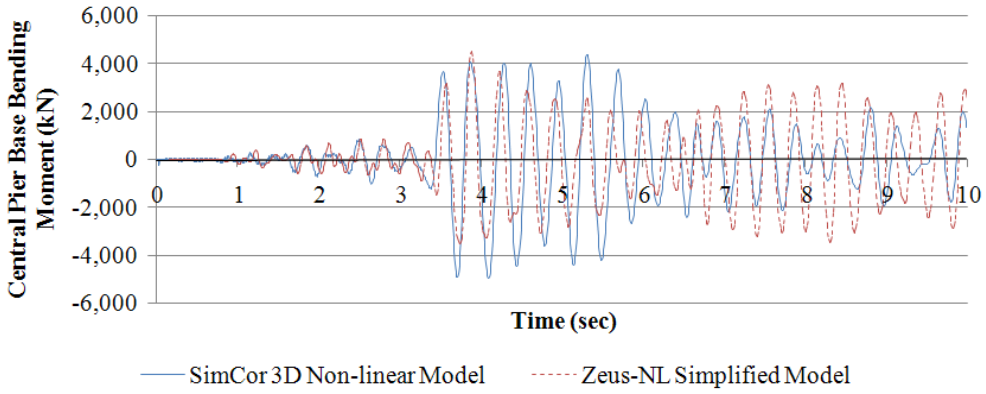

Figure 3 Dynamic response of the Central Pier using single and multi-platform analysis (excitation case: C22)

4. FRAGILITY ANALYSIS

4.1 Procedure to derive fragility relationships

Having defined the complete set of analysis cases and calibrated the non-linear finite element model to be used, a parametric scheme of 36x4=144 inelastic dynamic analyses was set. By assuming damage concentration solely at the bottom of the central pier, the pier *local* and bridge *global* Damage Indices (DI) were identical for each analysis and were computed based on the resulting Moment-Curvature curve and the modified Park-Ang relationship (Kunnath et al., 1997):

$$D_L = \frac{\varphi_m - \varphi_y}{\varphi_u - \varphi_y} + \beta_e \frac{E}{M_y \varphi_u} \quad (1)$$

where φ_m is the maximum curvature achieved during cyclic loading, φ_y and M_y is the yield curvature and bending moment of the concrete section respectively, E is the cumulative energy absorbed in the hysteresis loops and β_e a strength loss parameter set equal to 0.1 (Kunnath et al., 1997). After calculation of the median DI values for each level of intensity measure (i.e. bedrock PGA) and appropriate curve fitting, the Damage Index and Damage States were correlated according to Stone and Taylor (1993), i.e. damage limit state I ('repairable damage') was considered for values of 0.11<DI<0.40, damage limit state II ('irrepairable damage') for values 0.40<DI<0.77 and damage limit state III ('collapse') for 0.77<DI<1.00. Four different fragility curves were then derived corresponding to the above four analyses cases and the probability of exceeding a particular level of damage d_{si} was calculated assuming lognormal distribution (a global factor of β_{dsi} = 0.6 was used to account for all sources of demand and supply uncertainty).

4.2 Comparative assessment of the effect of liquefaction on bridge fragility

The resulting fragility relationships for each one of the three aforementioned damage states are illustrated in Figure 4. It is observed that due to the moderate abutment and pier foundation stiffness, the introduction of soil-foundation compliance at the supports of the MRO bridge affects has a less significant effect than liquefaction. Moreover, it is observed that the probability of exceeding the 'repairable' damage limit state (I) is generally independent of the scenario studied. This can be primarily attributed to the fact that both soil-structure interaction and liquefaction are response aspects which become important at higher levels of ground excitation.

On the contrary, the 'irreparable' damage limit state requires significantly higher levels of earthquake intensity (as expressed in terms of bedrock PGA) in comparison with the cases of either local or no liquefaction. The most important implication of spatially extensive liquefaction though, is that it essentially prevents the structure from reaching the critical 'collapse' limit state (III), since it reduces the imposed input accelerations to the level of the critical acceleration (0.25-0.29g). As a result, the corresponding fragility curve for 'collapse' does not exist. Such reduction of earthquake forces due to liquefaction is indeed in agreement with a number of recent studies (i.e. Adalier and Elgamal, 2002). Nevertheless, it is important to recall that the fragility curves are inevitably related to the selected damage mechanisms, which were related solely to the flexural

damage potential at the base of the Center Pier in this study. What is important to point out therefore, is that in case of liquefaction, the seismic demand in the MRO central pier may be significantly reduced. However, different and additional damage mechanisms could be activated such as extensive rocking at the soil–pier foundation interface, damaging pile bending strains at interfaces between soil layers of strong impedance contrast (i.e. successive liquefied and non-liquefied layers) or extensive movements at the abutments, all related to damage not captured by the methodology adopted herein. Along these lines, it is deemed that a more refined global damage index should be used to describe damage in case of liquefaction susceptible subsoils.

Another interesting aspect is the effect of the extent of liquefaction on the anticipated level of pier damage. As seen in Figure 4, when liquefaction is localized below the Centre Pier, the (flexural) damage at the pier base was found lower compared to the case where no liquefaction was considered (with all limitations presented above regarding the mechanisms considered), but clearly more critical than the 'global liquefaction' case. In other words, local liquefaction below Center Pier combines the unfavourable effects of large soil movements at its base, as described above (even if they are not reflected on the fragility curves derived), and the increased seismic demand observed in Figure 4 which can be attributed to two main reasons: (a) the abutments are not subjected to the critical acceleration of the liquefied ground below the central pier, hence, they essentially drive the motion of the bridge, while (b) the pier is subjected to additional pseudo-static forces arising from the asynchronous earthquake input, proven considerable, despite the short overall length of the bridge and the subsequent negligible phase lag of seismic waves.

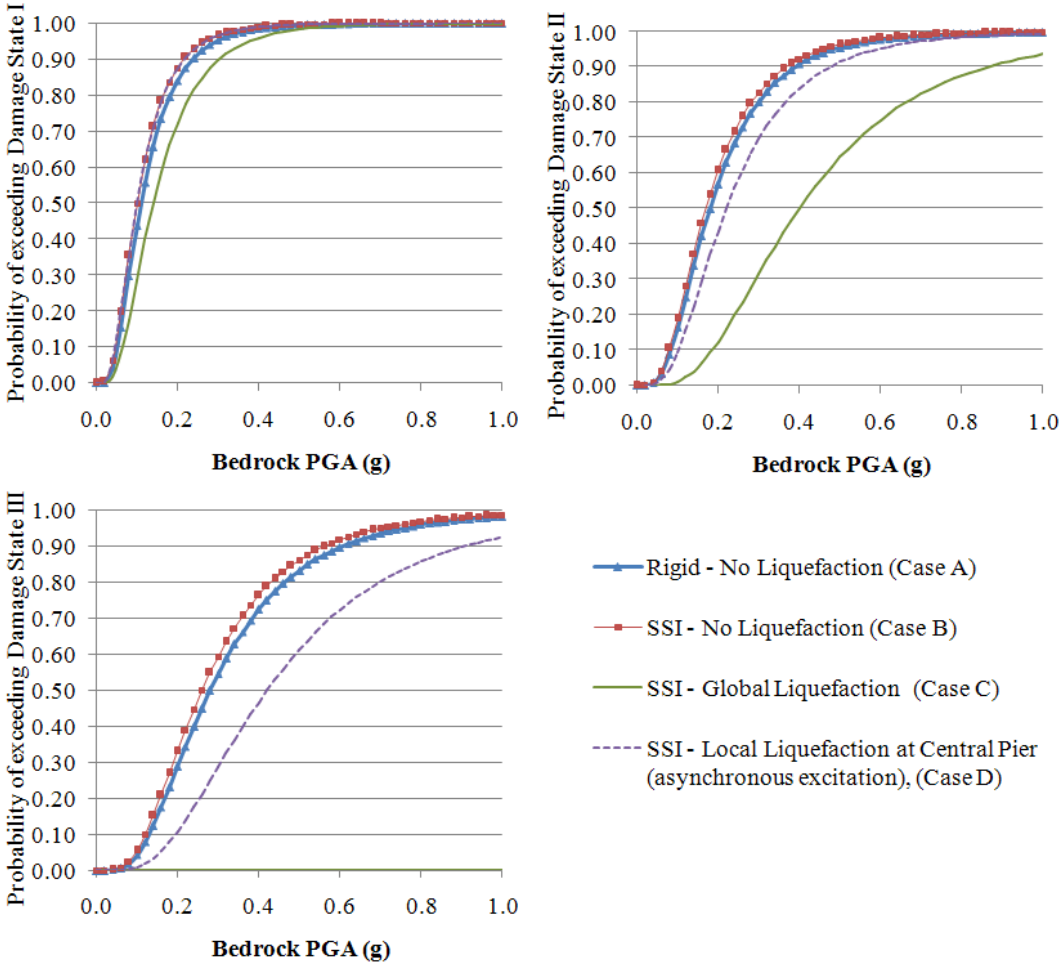

Figure 4 Fragility curves for the four foundation flexibility and excitation cases studied

5. CONCLUSSIONS

This paper reports an exploratory investigation of the effect of soil liquefaction on fragility relationships for a bridge-foundation-soil system. A refined computational scheme was implemented for this purpose involving both 3-D and simplified inelastic finite element models, detailed inelastic site response analyses considering liquefaction as well as uniform and incoherent earthquake input. The results of the study indicate that the inelastic dynamic response of the investigated bridge-foundation-soil system is significantly affected by the liquefaction of upper sand layers while the spatial extent of liquefaction is an additional parameter that has to be considered as an important source of ground motion and ductility demand variation. Further research is needed in order to investigate static and dynamic soil-structure interaction effects with emphasis on the role of the embankment on the abutment stiffness and input motion.

6. ACKNOWLEDGEMENTS

The contribution of the first author was sponsored by the Mid-America Earthquake Center, a National Science Foundation Engineering Research Center funded under grant reference EEC-9701785. The contribution of the third author was supported by the Federal Highway Administration, contract reference ALTD3-1-080205-3. The second author would also like to thank Prof. G. Manolis for his contribution regarding generation of ground motion scenarios.

7. REFERENCES

Adalier, K., and A.-W. Elgamal (2002). "Seismic response of adjacent dense and loose saturated columns", *Soil Dynamics and Earthquake Engineering*, Vol. 22, 115-127.

Ambraseys, N., and Douglas, J. (2000). "Reappraisal of the effect of vertical ground motions on response", ESEE Report 00-4. *Dept. of Civil and Env. Eng., Imperial College*, London.

Elgamal, A., Yang, Z. and Parra, E.(2002). "Computational Modeling of Cyclic Mobility and Post-Liquefaction Site Response.", *Soil Dynamics and Earthq. Eng.*, Vol. 22, No. 4, 259-271.

Elnashai, A. S., Papanikolaou, V., and Lee, D. (2002). "Zeus NL – A System for Inelastic Analysis of Structures." *Mid-America Earthquake Center, University of Illinois at Urbana-Champaign*, Program Release Sept. 2002.

Kwon, O. S., Nakata, N., Elnashai, A. S., and Spencer, B. (2005). "A Framework for Multi-Site Distributed Simulation and Application to Complex Structural Systems", *Journal of Earthquake Engineering*, Vol. 9, No. 5, 741-753.

Kwon, O.S. (2007). "Probabilistic Seismic Assessment of Structure, Foundation and Soil Interacting Systems", Ph.D. Thesis, University of Illinois at Urbana-Champaign.

Kunnath , S. El-Bahy, K., Taylor, A. and Stone, W. (1997). "Cumulative Seismic Damage of Reinforced Concrete Bridge Piers", *NCEER Report 97/0006*, SUNY, Buffalo, N.Y.

Manolis, G.D, Rangelov, T.V. and Dineva, P.S. (2007) "Free-field wave solutions in a half-plane exhibiting a special-type of continuous inhomogeneity", *Wave Motion* ,Vol. 44,No. 4, 304-321.

McGuire, R.K. (1978). "Seismic ground motion parameter relations", *Journal of the Geotechnical Engineering Division*, ASCE, 104(GT4), 481–490.

McKenna, F., and Fenves, G. L. (2001). "The OpenSees command language manual, version 1.2.", *Pacific Earthquake Engineering Research Center*, University of California at Berkeley.

Papageorgiou, A.S. and Aki, K. (1983) "A specific barrier model for the quantitative description of inhomogeneous faulting and the prediction of strong ground motion: I. Description of the model", *Bulletin Seismological Society of America,* Vol. 73, No. 3, 693-722.

Shinozuka, M. (1987). "Stochastic fields and their digital simulation, in Stochastic Methods in Structural Dynamics", Martinus Nijhoff, Dordrecht, The Netherlands.

Stone, W. C. and Taylor, A.W. (1993) "Seismic performance of circular bridge columns designed in accordance with AASHTO/CALTRANS standards", *NIST Building Science Series*, 170, National Institute of Standards and Technology, Gaithersburg, M.D.

Zhang, J. and Makris, N. (2001). "Seismic Response Analysis of Highway Overcrossings Including Soil-Structure Interaction", *PEER Research Report, 2001/02,* Berkeley, U.S.